Hindawi
Mathematical Problems in Engineering
Volume 2019, Article ID 7672623, 14 pages
https://doi.org/10.1155/2019/7672623

Research Article

A Kriging-Based Active Learning Algorithm for Mechanical Reliability Analysis with Time-Consuming and Nonlinear Response

Cao Tong,[1,2] **Jian Wang**,[3] **and Jinguo Liu**[2]

[1]*School of Mechatronics Engineering, Shenyang Aerospace University, Shenyang 110136, China*
[2]*State Key Laboratory of Robotics, Shenyang Institute of Automation, Chinese Academy of Sciences, Shenyang 110016, China*
[3]*School of Mechanical Engineering & Automation, Northeastern University, Shenyang 110819, China*

Correspondence should be addressed to Cao Tong; tongcao19@163.com

Received 8 April 2019; Revised 16 July 2019; Accepted 21 July 2019; Published 18 August 2019

Academic Editor: A. M. Bastos Pereira

When the reliability analysis of the mechanical products with high nonlinearity and time-consuming response is carried out, there will be the problems of low precision and huge computation using the traditional reliability methods. To solve these issues, the active learning reliability methods have been paid much attention in recent years. It is the key to choose an efficient learning function (such as U, EFF, and ERF). The aim of this study is to further decrease the computation and improve the accuracy of the reliability analysis. Inspired from these learning functions, a new point-selected learning function (called HPF) is proposed to update DOE, and a new point is sequentially added step by step to the DOE. The proposed learning function can consider the features like the sampling density, the probability to be wrongly predicted, and the local and global uncertainty close to the limit state. Based on the stochastic property of the Kriging model, the analytic expression of HPF is deduced by averaging a hybrid indicator throughout the real space. The efficiency of the proposed method is validated by two explicit examples. Finally, the proposed method is applied to the mechanical reliability analysis (involving time-consuming and nonlinear response). By comparing with traditional mechanical reliability methods, the results show that the proposed method can solve the problems of large computation and low precision.

1. Introduction

In the mechanical reliability analysis (MRA), when the joint probability density function $f_{\mathbf{X}}(\mathbf{x})$ of the random variable vector $\mathbf{X} = [X_1, X_2, \ldots, X_n]^{\mathrm{T}}$ is known, the failure probability can be expressed as

$$P_{\mathrm{f}} = P(g(\mathbf{x}) \le 0) = \int_{\mathrm{F}} f_{\mathbf{X}}(\mathbf{x})dx = \int I_{g\le 0}(\mathbf{x}) f_{\mathbf{X}}(\mathbf{x})dx, \tag{1}$$

where $g(\mathbf{x})$ is the performance function of the mechanical system. If $g(\mathbf{x}) > 0$, the system is in the safety state; otherwise, it is in the failure state. $I_{g\le 0}(\mathbf{x}) = \begin{cases} 1, & g(\mathbf{x}) \le 0, \\ 0, & g(\mathbf{x}) > 0, \end{cases}$ and the failure domain F and the safety domain S of input random variables are $F = \{\mathbf{x} \mid g(\mathbf{x}) \le 0\}$ and $S = \{\mathbf{x} \mid g(\mathbf{x}) > 0\}$, respectively.

However, the performance function $g(\mathbf{x})$ of the MRA is obtained by solving the numerical model (such as finite element method and finite different method) which is usually time-consuming and highly nonlinear. For this situation, the moment reliability methods [1] are not applicable because the calculated reliability's accuracy is very low due to ignorance of the Taylor expansion's high-order items. While the random simulation methods [2, 3] (such as Monte Carlo simulation (MCS), important sampling (IS), subset simulation (SS), line sampling (LS), and Latin hypercube sampling) are unaffordable because their calculation computation is too huge for calling a large of numerical models. It also takes too much time to

calculate the reliability by the workstation computer. Therefore, in MRA, it is the core problem to minimize the number of calls to the numerical calculation under the premise of ensuring the calculated accuracy.

To solve the problem of large computation in MRA, several surrogate models (including polynomial response surfaces [1], sparse polynomials [4], neural networks [5], support vector machines [6], and Kriging [7]) are usually replaced with the real performance function. Since the speed of calculating the surrogate function is much faster than the real performance function, the surrogate model techniques are widely applied to MRA. However, there are two weaknesses in these surrogate model techniques: firstly, the sample points of the design of experiment (DOE) must be arranged in advance before the surrogate model of the performance function is constructed. This fixed DOE's scheme will cause excessive sampling of areas where design variables are not important and then results in unnecessary computational waste. Secondly, the traditional surrogate-based reliability methods only guarantee that the fitting performance function is as accurate as possible, while the accuracy of the reliability analysis cannot be guaranteed.

Kriging, as a surrogate model, shows better fitting accuracy than other surrogate models [4, 8, 9]. Kriging not only is a interpolation model but also provides the mean and variance at an unknown point. Because of the statistical information of Kriging, the Kriging-based active learning reliability method (KARM) has received much attention in the recent years. The basic idea of KARM is to sequentially refresh the DOE, and the constructed surrogate model gradually reaches to the real performance function. Inspired by the famous efficient global optimization (EGO) method [10], Bichon et al. [11, 12] proposed an efficient global reliability analysis (EGRA) method to search the DOE's points in the vicinity of the limit state. Echard et al. proposed an active learning reliability method (AK-MCS/AK-IS) [13, 14] by combing MCS/IS and Krigng. Yang et al. [15] proposed a reliability mixed algorithm (ALK-HRA) based on probability and convex set hybrid reliability analysis. Wen et al. [16] proposed a dynamic sampling area strategy (SKRA) to avoid selecting samples in areas with low probability density, to improve the efficiency of selecting the best point. Among these methods, AK-MCS [13] is one of the most typical KARMs, whose learning function U is an innovative point-selected learning function that measures the probability of classifying a point into the wrong domain. Based on AK-MCS, there are many scholars who have extended the study of U in order to solve some special conditions (such as small failure probability, multiple dimension, multiple failure regions, and systems) of reliability analysis. For example, Echard et al. [14] combined the AK-MCS algorithm idea with IS (AK-IS) to make it suitable for solving the reliability problem with small failure probability. Tong et al. [17] combined the AK-MCS idea with the SSIS method for the small failure probability problem, to improve the robustness of multidimensional random variables. Cadini et al. [18] improved the AK-IS to solve the reliability problem of multiple areas and small failure probability. Fauriat and Gayton [19] presented the AK-SYS method which is adaptation to system problems.

Many studies [20–23] indicated that it is the key problem to choose a good learning function for guiding the DOE's strategy of KARM. Some efficient learning functions have been presented in recent years. Yang et al. [20] defines the expected risk function (ERF), which provides an indication of how large the predicted performance function value is if the sign of the predicted performance function is wrongly predicted. Lv et al. [21] proposed a new learning function based on information entropy theory and applied it to the reliability algorithm in combination with the LS method. Sun et al. [22] proposed a learning function that considers the degree of improvement in prediction accuracy and probability density based on a dynamic point selection update strategy and established a relatively high-precision Kriging prediction model relatively quickly. Wang and Sun [23] roughly determined the region where $g(\mathbf{x}) = 0$ according to Kriging prediction statistics and gradually increased the number of sample points in the region to maximize a certain accuracy index of the Kriging model.

The aim of this paper is to further decrease the computation and improve the accuracy of reliability analysis. A Kriging-based active learning reliability method is presented, in which an efficient point-selected learning function (called HPF) is proposed to update DOE. The uncertainty of HPF could measure the features like the sampling density, the probability to be wrongly predicted, and the local and global uncertainties close to the limit state. The new point-selected learning function can help select the next point effectively, and only a small number of real performance function evaluations are required to build an accurate Kriging performance function. Finally, the gear reliability analysis is taken as the object of this study, whose performance function response's behavior is nonlinear and time-consuming. It is a difficult task that gear reliability is evaluated accurately and efficiently by traditional mechanical reliability methods (such as crude MCS, FORM, and RSM). The proposed method is applied to the reliability analysis of gear. This study will provide reference for the reliability design of the gear vibration.

This article is organized as follows: Section 2 introduces the structural reliability method based on the Kriging surrogate model and Monte Carlo simulation. Section 3.1 presents a new hybrid point-selected learning function and then describes the analytic expression of HPF. Section 3.2 describes the procedures of the proposed Kriging-based active reliability method. Section 4 illustrates the efficiency and correctness of the proposed method through two academic examples. In Section 5, the proposed method is applied to analyze the reliability analysis of gear. Section 6 is the conclusion.

2. Kriging Surrogate Model for Structural Reliability Analysis

Following [4], the Kriging response $g(\mathbf{x})$ can be expressed as

$$g(\mathbf{x}) = \sum_{i}^{p} \boldsymbol{\beta}_i k_i(\mathbf{x}) + z(\mathbf{x}) = \mathbf{k}(\mathbf{x})^{\mathrm{T}} \boldsymbol{\beta} + z(\mathbf{x}), \tag{2}$$

where $\boldsymbol{\beta}$ is the vector of regression coefficient; $\mathbf{k}(\mathbf{x})$ is the vector of polynomial, where constant polynomials are selected as the basic functions; and $z(\mathbf{x})$ is the random process, and the covariance of $z(\mathbf{x})$ is

$$E(z(\mathbf{w})z(\mathbf{x})) = \sigma^2\mathbf{R}(\boldsymbol{\theta}, \mathbf{w}, \mathbf{x}), \tag{3}$$

where σ^2 is the variance of the process and $\mathbf{R}(\boldsymbol{\theta}, \mathbf{w}, \mathbf{x})$ is the correlation function between $z(\mathbf{w})$ and $z(\mathbf{x})$, where a Gaussian correlation function is selected as

$$R(\boldsymbol{\theta}, \mathbf{w}, \mathbf{x}) = \prod_{k}^{n} R_k(\boldsymbol{\theta}_k, \mathbf{w}_k, \mathbf{x}_k) = \exp\left(-\sum_{k=1}^{n} \boldsymbol{\theta}_k |\mathbf{w}_k - \mathbf{x}_k|^2\right). \tag{4}$$

Under the consideration of linear predictor, the predictor at the unobserved point $\mathbf{x}$ is a normal distribution variable before calculating the true response. And the predictor follows a Gaussian distribution:

$$g(\mathbf{x}) \sim N[\widehat{g}(\mathbf{x}), s(\mathbf{x})], \tag{5}$$

where the Kriging predictor value $\widehat{g}(\mathbf{x})$ and standard variance $s(\mathbf{x})$ can be expressed as

$$\mu(\mathbf{x}) = \widehat{g}(\mathbf{x}) = \mathbf{k}(\mathbf{x})^{\mathrm{T}}\boldsymbol{\beta}^* + \mathbf{r}(\mathbf{x})^{\mathrm{T}}\mathbf{R}^{-1}(\mathbf{Y} - \mathbf{F}\boldsymbol{\beta}^*), \tag{6}$$

$$s^2(\mathbf{x}) = \sigma_Z\left(1 + \mathbf{u}(\mathbf{x})^{\mathrm{T}}\left(\mathbf{F}^{\mathrm{T}}\mathbf{R}^{-1}\mathbf{F}\right)^{-1}\mathbf{u}(\mathbf{x}) - \mathbf{r}(\mathbf{x})^{\mathrm{T}}\mathbf{R}^{-1}\mathbf{r}(\mathbf{x})\right), \tag{7}$$

where $\boldsymbol{\beta}^*$ is the regression parameters of generalized least squares solution; $\mathbf{R}$ is the matrix of stochastic-process correlations between design sites; and $\mathbf{R} = [\mathbf{R} \cdot ij]\ m \times m$, where $\mathbf{R} \cdot ij = \mathbf{R}(\boldsymbol{\theta}, \mathbf{s}\ i, \boldsymbol{\theta}\ j)$, $i, j = 1, \cdots, m$; $\mathbf{r}(\mathbf{x}) = [\mathbf{R}(\boldsymbol{\theta}, \mathbf{s}_1, \mathbf{x})\ R(\boldsymbol{\theta}, \mathbf{s}_2, \mathbf{x}) \ldots \mathbf{R}(\boldsymbol{\theta}, \mathbf{s}_m, \mathbf{x})]^{\mathrm{T}}$; $\mathbf{u}(\mathbf{x}) = \mathbf{F}^{\mathrm{T}}\mathbf{R}^{-1}\ \mathbf{r} - \mathbf{k}$; $\sigma_z = (\mathbf{Y} - \mathbf{F}\boldsymbol{\beta}^*)^{\mathrm{T}}(\mathbf{Y} - \mathbf{F}\boldsymbol{\beta}^*)/m$.

The optimal coefficients $\boldsymbol{\theta}^*$ corresponding to maximum likelihood estimation should solve

$$\min_{\boldsymbol{\theta}}\left\{\psi(\boldsymbol{\theta}) \equiv |\mathbf{R}|^{1/m}\sigma^2\right\}, \tag{8}$$

where $|\mathbf{R}|$ is the determinant of $\mathbf{R}$.

When $\boldsymbol{\theta}^*$ is found, a Kriging prediction model can be established.

Then, the Kriging surrogate expression $\widehat{g}(\mathbf{x})$ will be substituted for the performance function $g(\mathbf{x})$ to calculate the failure probability, and it is used to calculate the failure probability:

$$p_{\mathrm{f}} \approx \widehat{p}_{\mathrm{f},\widehat{g}} = \int I_{\widehat{g}\le 0}(\mathbf{x}) f_X(\mathbf{x}) dx. \tag{9}$$

Because $\widehat{g}(\mathbf{x})$ is explicit expression, the computer can complete the calculation of the performance function $g(\mathbf{x})$ at millions of sample points in a short time. Therefore, Monte Carlo simulation, as the most common and robust method, is applied to reliability analysis in this paper. The failure probability can be expressed as

$$p_f = \frac{1}{n_{\mathrm{MCS}}}\sum_{i=1}^{n_{\mathrm{MCS}}} I_g\left(\mathbf{x}^i\right) = \frac{n_{g\le 0}}{n_{\mathrm{MCS}}}, \tag{10}$$

where $\mathbf{x} = [x_1, x_2, \cdots, x_n]^{\mathrm{T}}$ is the vector of input random variables with n-dimension in the domain; $f_{\mathbf{X}}(\mathbf{x})$ is the joint probability density function of $\mathbf{x}$; n_{MCS} is the number of random samples generated by MCS; $\mathbf{x}_i$, $(i = 1, 2, \ldots, n_{\mathrm{MCS}})$ is the ith sample in the Monte Carlo population; $I_g(\mathbf{x})$ is a indicator function, and it can be defined as

$$I_g(\mathbf{x}) = \begin{cases} 0, & \text{when } g(\mathbf{x}) \le 0, \\ 1, & \text{when } g(\mathbf{x}) > 0. \end{cases} \tag{11}$$

The coefficient of variation of $\widehat{p}_{\mathrm{f},g}$ is calculated as

$$\delta = \sqrt{\frac{1 - \widehat{p}_{\mathrm{f},g}}{n_{\mathrm{MCS}}\widehat{p}_{\mathrm{f},g}}}. \tag{12}$$

3. Kriging-Based Active Learning Reliability Method

3.1. Point-Selected Learning Function. The idea of the Kriging-based active learning reliability method (KARM) is to perform a relatively small DOE and sequentially add a new point step by step to the DOE, and then the constructed Kriging surrogate model gradually approaches to the real performance function. So the surrogate model is to be replaced with the real performance function when reliability analysis is conducted. Studies show that the key of the Kriging-based active learning reliability method is to choose an efficient point-selected learning function, where some widely used learning functions consist of such as EFF [11], U [13], and ERF [15]. Inspired by the own advantages of these efficient learning functions, combination of some efficient features is proposed and deduced to further improve the efficiency and accuracy of the KARM. The proposed learning function (called "HPF") could consider the features like the sampling density, the probability to be wrongly predicted, and the local and global uncertainty close to the limit state. And, the derivation of HPF is elaborated below.

Firstly, based on equation (5) of Kriging theory in Section 2, $g(\mathbf{x})$ is assumed to a random variable and $g(\mathbf{x}) \sim N[\widehat{g}(\mathbf{x}), s(\mathbf{x})]$ under the Kriging framework. As shown in Figure 1, $f_g[\mathrm{g}(\mathbf{x})]$ is the probability density and $\widehat{g}(\mathbf{x})$ and $s(\mathbf{x})$are the Kriging predictor value and standard variance, to equation (1), the failure probability p_{f} is only related to the positive or negative of the state function $g(\mathbf{x})$ instead of the absolute value of $g(\mathbf{x})$ in the $\mathbf{X}$ domain. The accuracy of the Kriging-based reliability analysis can be interpreted as the accuracy of $\widehat{g}(\mathbf{x}) = 0$ relative to $g(\mathbf{x}) = 0$. As shown in Figure 2, $\widehat{g}(\mathbf{x}) = 0$ and $g(\mathbf{x}) = 0$ divide the $\mathbf{X}$ space into four parts: the signs of $\widehat{g}(\mathbf{x})$ and $g(\mathbf{x})$ in the domain D_1 and D_3 are the same and the signs of $\widehat{g}(\mathbf{x})$ and $g(\mathbf{x})$ in the domain D_2 and D_4 are converse. The probability that the sign of $\widehat{g}(\mathbf{x})$ is opposite to the sign of $g(\mathbf{x})$ can be expressed as

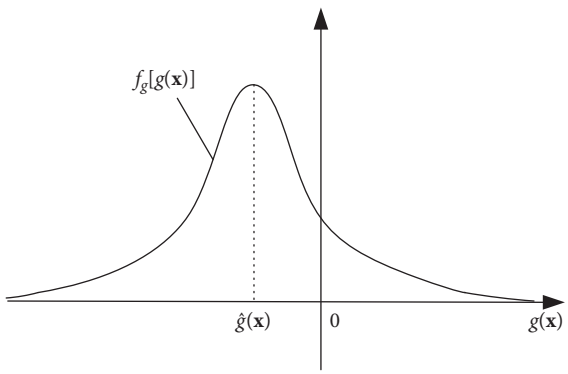

Figure 1: Probability density function of $g(\mathbf{x})$.

$$\text{Error} = \int_{D_2 \cup D_4} f_{\mathbf{X}}(\mathbf{x})dx = \int \left| I_{g\le 0}(\mathbf{x}) - I_{\widehat{g}_{\le 0}}(\mathbf{x}) \right| f_{\mathbf{X}}[\mathbf{x}]dx. \tag{13}$$

In the Kriging framework, the predicted sign at the point $\mathbf{x}$ is a random variable $I_{g\le 0}(\mathbf{x})$, and $I_{g\le 0}(\mathbf{x})$ obeys the distribution of 0-1 with the parameter $U_g(\mathbf{x}) = |\widehat{g}(\mathbf{x})/s(\mathbf{x})|$. According to [24], the accuracy of $\widehat{p}_{\mathrm{f}}$ can be measured as

$$E_g = E[\text{Error}] = \int \Phi\left(-U_g(\mathrm{x})\right) \cdot f_{\mathbf{X}}[\mathbf{x}]dx. \tag{14}$$

It is shown from equation (14) that the larger the value of $\Phi(-U_g(\mathbf{x})) \cdot f_{\mathbf{X}}(\mathbf{x})$ is, the larger is the accuracy of probability of predicting $g(\mathbf{x})$ to be wrong, where $U_g(\mathbf{x})$ is the learning function of AK-MCS [13] and $f_{\mathbf{X}}(\mathbf{x})$ indicates the sampling points' density; so $\Phi(-U_g(\mathbf{x})) \cdot f_{\mathbf{X}}(\mathbf{x})$ will be regarded as one part of the proposed indication function.

Secondly, as shown in Figure 3(a), the larger the value of $\mathrm{RF}(g(\mathbf{x})) = \begin{cases} \max\{g(\mathbf{x}) - 0, 0\}, & \widehat{g}(\mathbf{x}) < 0, \\ \max\{0 - g(\mathbf{x}), 0\}, & \widehat{g}(\mathbf{x}) \ge 0, \end{cases}$ [15] is, the higher the uncertainty of the corresponding sample point in the global area is. According to [11], the point with the larger value of $\mathrm{EF}(g(\mathbf{x})) = \max\{\varepsilon - |g(\mathbf{x})|, 0\}$ is to be the higher uncertainty in local region $(-\varepsilon, \varepsilon)$, which is shown in Figure 3(b). Therefore, $\mathrm{RF}(g(\mathbf{x})) \cdot \mathrm{EF}(g(\mathbf{x}))$ could balance the local and global uncertainty of $g(\mathbf{x})$, and then it measures the uncertainty more reasonably.

However, $\mathrm{RF}(g(\mathbf{x})) \cdot \mathrm{EF}(g(\mathbf{x}))$ is a random variable, so the expectation of $\mathrm{RF}(g(\mathbf{x})) \cdot \mathrm{EF}(g(\mathbf{x}))$ is used to measure this uncertainity. Just like EFF [11] and ERF [15], we average $\mathrm{RF}(g(\mathbf{x})) \cdot \mathrm{EF}(g(\mathbf{x}))$ throughout the real space. So $E[\mathrm{RF}(g(\mathbf{x})) \cdot \mathrm{EF}(g(\mathbf{x}))]$ is expressed as

$$\begin{aligned} E[\mathrm{RF}(g(\mathbf{x})) \cdot \mathrm{EF}(g(\mathbf{x}))] &= \int_{-\infty}^{+\infty} \mathrm{RF}(g(\mathbf{x})) \cdot \mathrm{EF}(g(\mathbf{x})) f_{g(\mathbf{x})} \\ &\quad [g(\mathbf{x})]dg(\mathbf{x}) \\ &= \begin{cases} \displaystyle\int_{-\varepsilon}^{0} \max\{g(\mathbf{x}) - 0, 0\} \cdot \max\{\varepsilon - |g(\mathbf{x})|, 0\} f_{g(\mathbf{x})}[g(\mathbf{x})]dg(\mathbf{x}) \\ \displaystyle\int_{0}^{\varepsilon} \max\{0 - g(\mathbf{x}), 0\} \cdot \max\{\varepsilon - |g(\mathbf{x})|, 0\} f_{g(\mathbf{x})}[g(\mathbf{x})]dg(\mathbf{x}). \end{cases} \end{aligned} \tag{15}$$

This integral is expressed analytically as (the derivation process can be seen in Appendix)

$$\begin{aligned} E[\mathrm{RF}(g(\mathbf{x})) \cdot \mathrm{EF}(g(\mathbf{x}))] = -\mathrm{sign}(\widehat{g}(\mathbf{x})) \Bigg\{ & [\widehat{g}(\mathbf{x})(-\varepsilon \mathrm{sign}(\widehat{g}(\mathbf{x})) \\ & - \widehat{g}(\mathbf{x}))s(\mathbf{x})] \cdot \left[\Phi\left(\frac{-\varepsilon \mathrm{sign}(\widehat{g}(\mathbf{x})) - \widehat{g}(\mathbf{x})}{s(\mathbf{x})} \right) \right. \\ & \left. - \Phi\left(\frac{-\widehat{g}(\mathbf{x})}{s(\mathbf{x})} \right) \right] + \widehat{g}(\mathbf{x}) s(\mathbf{x}) \varphi \\ & \cdot \left(\frac{-\varepsilon \mathrm{sign}(\widehat{g}(\mathbf{x})) - \widehat{g}(\mathbf{x})}{s(\mathbf{x})} \right) + s(\mathbf{x}) \\ & \cdot [-\varepsilon \mathrm{sign}(\widehat{g}(\mathbf{x})) - \widehat{g}(\mathbf{x})] \varphi\left(\frac{-\widehat{g}(\mathbf{x})}{s(\mathbf{x})} \right) \Bigg\}, \end{aligned} \tag{16}$$

where $\mathrm{sign}(\cdot)$ is the sign function and $\mathrm{sign}(\widehat{g}(\mathbf{x})) = \begin{cases} 1, & \widehat{g}(\mathbf{x}) \ge 0, \\ -1, & \widehat{g}(\mathbf{x}) < 0. \end{cases}$

Above all, a hybrid point-selected function (HPF) is defined as

$$\begin{aligned} \mathrm{HPF}(\mathbf{x}) = -\mathrm{sign}(\widehat{g}(\mathbf{x})) f_{\mathbf{X}}(\mathbf{x}) \Phi\left(-\left| \frac{\widehat{g}(\mathbf{x})}{s(\mathbf{x})} \right| \right) \Bigg\{ & [g(\mathbf{x}) \\ & \cdot (-\varepsilon \mathrm{sign}(\widehat{g}(\mathbf{x})) - \widehat{g}(\mathbf{x}))s(\mathbf{x})] \\ & \cdot \left[\Phi\left(\frac{-\varepsilon \mathrm{sign}(\widehat{g}(\mathbf{x})) - \widehat{g}(\mathbf{x})}{s(\mathbf{x})} \right) - \Phi\left(\frac{-\widehat{g}(\mathbf{x})}{s(\mathbf{x})} \right) \right] \\ & + \widehat{g}(\mathbf{x}) s(\mathbf{x}) \varphi\left(\frac{-\varepsilon \mathrm{sign}(\widehat{g}(\mathbf{x})) - \widehat{g}(\mathbf{x})}{s(\mathbf{x})} \right) \\ & + s(\mathbf{x}) [-\varepsilon \mathrm{sign}(\widehat{g}(\mathbf{x})) - \widehat{g}(\mathbf{x})] \varphi\left(\frac{-\widehat{g}(\mathbf{x})}{s(\mathbf{x})} \right) \Bigg\}, \end{aligned} \tag{17}$$

where $\widehat{g}(\mathbf{x})$ and $s(\mathbf{x})$ are the Kriging predictor value $\widehat{g}(\mathbf{x})$ and standard variance $s(\mathbf{x})$ seen in equations (6) and (7), respectively; $\Phi(\cdot)$ and $\varphi(\cdot)$ are the cumulative distribution function and the probability density function of the standard normal distribution, respectively; $\varepsilon = k \cdot s(\mathbf{x})$ and $k = 3$ is selected in this paper; $\mathrm{sign}(\cdot)$ is the sign function, and $\mathrm{sign}(\widehat{g}(\mathbf{x})) = \begin{cases} 1, & \widehat{g}(\mathbf{x}) \ge 0, \\ -1, & \widehat{g}(\mathbf{x}) < 0. \end{cases}$ Note that equation (17) is hereafter referred to as 'HPF' in this study because HPF is the abbreviation of the hybrid point-selected function.

3.2. Stopping Criterion. The stopping criterion directly determines the number of calls to the real performance function (referred to as 'n_{call}'). If n_{call} is too small, the accuracy of the constructed surrogate model is too low; while if n_{call} is too large, the computation is too large. Therefore, it is the key point to choose a precise and efficient criterion in the active learning reliability methods.

In AK-MCS [13], the stopping criterion can be expressed as

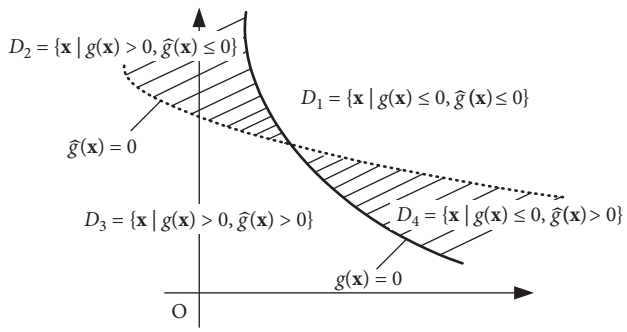

Figure 2: Illustration of the accuracy of $\hat{g}(\mathbf{x}) = 0$.

$$\min_{\mathbf{x}\in\mathbf{S}} (U(\mathbf{x})) \ge 2, \tag{18}$$

where $U(\mathbf{x})$ is the learning function of AK-MCS [13], $U(\mathbf{x}) = |\hat{g}(\mathbf{x})/s(\mathbf{x})|$, $\mathbf{S}$ is the sampling points of MCS, and $\mathbf{S} = \{\mathbf{x}^1, \mathbf{x}^2, ..., \mathbf{x}^{n_{\text{MCS}}}\}$.

The stopping criterion $\min_{\mathbf{x}\in\mathbf{S}} (U(\mathbf{x})) \ge 2$ only considers the sampling point with the worst predicting accuracy. It does not consider the prediction accuracy of all sampling points of MCS. This stopping criterion is too rough and not rigorous. In order to more accurately predict the sign of all sampling points, a stopping criterion considering global samples is presented in the literature [25], namely,

$$P(C) \ge 0.99, \tag{19}$$

where the event C denotes all the points of the MCS population are correctly classified, and $P(C) = \prod_{i=1}^{n_{\text{MCS}}} \Phi(|\hat{g}(\mathbf{x}^i)/s(\mathbf{x}^i)|)$.

The stopping criterion $P(C) \le 0.99$ means that the probability that all the points are correctly classified is greater than 0.99. It requires that the prediction accuracy of every point of the MCS population is more accurate. For example, if the prediction accuracy of every point of the 10^5 MCS population is assumed as $P(C_i) = 0.99999$, the probability that all points are correctly classified should be $P(C) = \prod_{i=1}^{100000} 0.99999 = 0.36788$. Or there is only one sampling point with $P(C_i) < 0.99$; the active learning process will not stop. Therefore, this stopping criterion is so strict that the accuracy of the calculated failure probability is very high, but it also requires more iterations. Especially when the real performance function is time-consuming, the calculation of the active learning reliability method is too large.

In order to avoid above problems of the classical stopping criteria, an improved stopping criterion is adopted in this paper. This criterion is based on the fact that the signs of all sampling points are independent, and it could consider the global sampling points as well. This stopping criterion is not affected by a few local points with the low prediction accuracy (such as $P(C_i) < 0.99$). Therefore, it can get a relatively acceptable results faster than others. The improved stopping condition is presented as (the derivation process and more details can be found in the literature [17])

$$\begin{cases} \text{if any of } N_c^k \ge \dfrac{P_{\text{threshold}} n_{\text{MCS}}}{P_{\text{control}}^k}, \quad k = 1, 2, \ldots, n_c, \\ \\ \text{then iteration stops,} \end{cases} \tag{20}$$

where $P_{\text{threshold}}$ is the threshold probability of classifying the right sign on $\mathbf{S}$; if $P_{\text{threshold}} = 0.998$, it means that the probability of predicting a right sign on population $\mathbf{S}$ is 0.998 at least; $P_{\text{control}}^k (k = 1, 2, ..., n_c)$ are uniformly distributed in $[P_{\text{threshold}}, 1)$, and the larger the n_c is, the more accurately the stopping condition (20) will judge the state of population (n_c equals to 100 in this paper); $N_c^k = \{\text{the number of } P^i > P_{\text{control}}^k \mid P^i \in P\}$, where $\mathbf{P} = \{P^1, P^2, \ldots, P^{n_{\text{MCS}}}\}$ is the vector corresponding to $\mathbf{S} = \{\mathbf{x}^1, \mathbf{x}^2, \ldots, \mathbf{x}^{n_{\text{MCS}}}\}$, e.g., $P^i = \Phi(U(x^i))$.

To better express how to use the stopping criterion, the judgment process of the stopping criterion is illustrated as follows. After each updating the Kriging prediction model, the following process is conducted.

Firstly, the probabilities of making a right sign at all sampling points are calculated by the current Kriging prediction model, and $P = \{P^1, P^2, \ldots, P^{n_{\text{MCS}}}\}$, $P^i = \Phi(U(\mathbf{x}^i))(i = 1, 2, ..., n_{\text{MCS}})$.

Secondly, $P_{\text{control}}^k (k = 1, 2, ..., n_c)$ are uniformly selected from the interval $[P_{\text{threshold}}, 1)$, and they are P control$^1 = P_{\text{threshold}}$, $P_{\text{control}}^2 = P_{\text{threshold}} + 1 \times (1 - P_{\text{threshold}})/n_c, \ldots, P_{\text{control}}^{n_c} = P_{\text{threshold}} + (n_c - 1) \times (1 - P_{\text{threshold}})/n_c$, respectively.

Thirdly, $N_c^k (k = 1, 2, \ldots, n_c)$ are calculated. For example, in case of $k = 1$, the number of sample points whose P^i is greater than P_{control}^1, where $\mathbf{P} = \{P^1, P^2, \ldots, P^{n_{\text{MCS}}}\}$ is the vector corresponding to $\mathbf{S} = \{\mathbf{x}^1, \mathbf{x}^2, \ldots, \mathbf{x}^{n_{\text{MCS}}}\}$, e.g., $P^i = \Phi(\mathbf{x}^i)$ $(i = 1, 2, ..., n_{\text{MCS}})$. In the similar way, when $k = 2, 3, ..., n_c$, N_c^2, N_c^3, ... $N_c^{n_c}$ are calculated, respectively.

Finally, on the basis of $P_{\text{control}}^k (k = 1, 2, ..., n_c)$ and $N_c^k (k = 1, 2, \ldots, n_c)$, respectively, judge whether $N_c^1 \ge P_{\text{threshold}} n_{\text{MCS}}/P_{\text{control}}^1$?, $N_c^2 \ge P_{\text{threshold}} n_{\text{MCS}}/P_{\text{control}}^2$?, ..., $N_c^{n_c} \ge P_{\text{threshold}} n_{\text{MCS}}/P_{\text{control}}^{n_c}$? If any of $N_c^k \ge P$ threshold$n_{\text{MCS}}/P_{\text{control}}^k$, $k = 1, 2, \ldots, n_c$ is meet, then the iteration would stop.

3.3. Procedures in the Present Study. The procedure (Figure 4) of the proposed active learning reliability method can be described as follows:

Step 1. Generate a Monte Carlo population $\mathbf{S} = \{\mathbf{x}^1, \mathbf{x}^2, \ldots, \mathbf{x}^{n_{\text{MCS}}}\}$ in the design space. At this stage, none of them is evaluated on the real performance function $g(\mathbf{x})$, and they are regarded as the candidate points to be evaluated on the real performance if KARM requires it.

Step 2. Define the initial DOE $\mathbf{S}_{\text{DOE}} = [\mathbf{p}^{(1)}, \ldots, \mathbf{p}^{(N)}]^{\text{T}}$ with small size $(N \ge (n + 1)(n + 2)/2$, in which n is the number of random variables over the bounds $\pm$ five standard deviations, and calculate $\mathbf{Y}_{\text{DOE}} = [\mathbf{y}^{(1)}, \ldots, \mathbf{y}^{(N)}]^{\text{T}}$ corresponding to $\mathbf{S}_{\text{DOE}}$ with the real performance function $g(\mathbf{x})$.

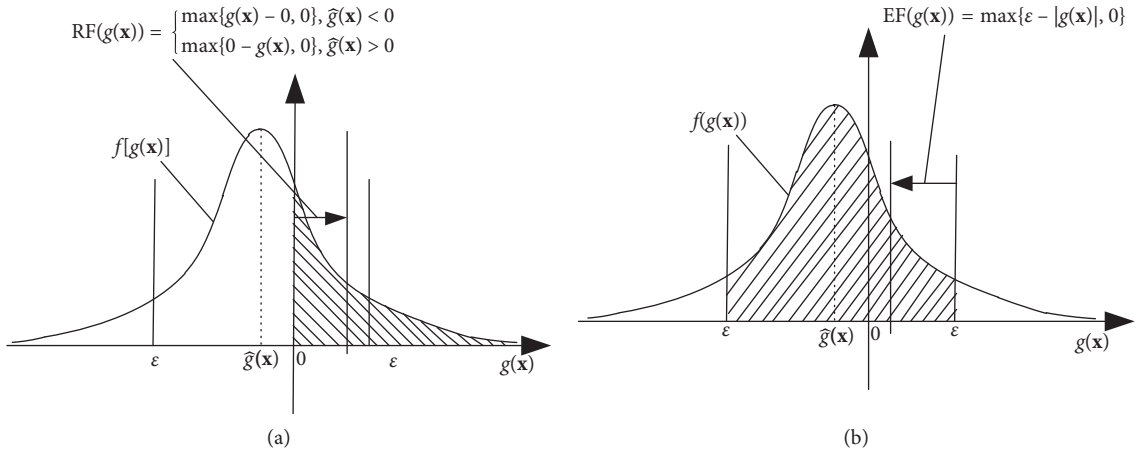

Figure 3: Uncertainty of different Kriging-based indications: (a) RF($g(\mathbf{x})$); (b) EF($g(\mathbf{x})$).

Step 3. Construct an Kriging predicted function model $\widehat{g}(\mathbf{x})$ from the $\mathbf{S}_{\mathrm{DOE}}$ and $\mathbf{Y}_{\mathrm{DOE}}$.

Step 4. Identify the best point $\mathbf{x}^*$ by the proposed HPF which is shown in equation (19). The HPF criterion of finding the best point is expressed as

$$\mathbf{x}^* = \arg\max_{\mathbf{x}\in\mathbf{S}} (\mathrm{HPF}(\mathbf{x})). \tag{21}$$

Step 5. Predict the performance function value $\widehat{g}(\mathbf{x}^i)$, $i = 1, \ldots, n_{\mathrm{MCS}}$, and estimate the failure probability $\widehat{p}_{\mathrm{f},\widehat{g}}$ and its coefficient of variation δ according to equations (10) and (12), respectively.

Step 6. If the stopping condition (equation (20)) is satisfied, stop iteration and go to Step 7; otherwise, $N = N + 1$, and update the previous DOE with the best point $\mathbf{x}^*$, and go to Step 3.

Step 7. If $\delta \le 0.03$, stop iteration and go to Step 8; otherwise, the population $\mathbf{S}$ enlarges and go to Step 3.

Step 8. Output the results.

4. Validation

4.1. Case 1 (Modified Rastrigin Function). This explicit example taken from [13, 18] is used to validate the efficiency and correctness of the proposed method. And, its performance function is a modified Rastrigin function, which is highly nonlinear involving nonconvex and nonconnex domains of failure. And, the performance function can be expressed as

$$g(\mathbf{x}) = 10 - \sum_{i=1}^{2}\left(x_i^2 - 5\cos\left(2\pi x_i\right)\right), \tag{22}$$

where $\mathbf{x} = [x_1, x_2]^{\mathrm{T}}$ is the vector of input random variables and x_1 and x_2 are standard normal distributed random variables, and they are independent.

This example is performed by the active learning reliability method (which can be seen in Section 3.3). Firstly, 10 points are sampled by the Latin hypercube sampling method as the initial DOE, and 10^5 points (called population $\mathbf{S}$) generated by MCS are regarded as the candidate points. The failure probability estimated by crude MCS, which is calling the real performance function, is regarded as the "true" solution (called it $\widehat{p}_{\mathrm{f},g}$ in this paper). Figure 5 shows the iterative process of the evaluated $\widehat{p}_{\mathrm{f},\widehat{g}}$. As the number of DOE's points increases, the estimated failure probability $\widehat{p}_{\mathrm{f},\widehat{g}}$ converges to the true one $\widehat{p}_{\mathrm{f},g}$. It takes about 281 points to obtain the failure probability $\widehat{p}_{\mathrm{f},\widehat{g}}$ with relative high accuracy. Figure 6 shows the initial DOE's points, iterative DOE's points, and the Kriging predicted function $\widehat{g}(\mathbf{x})$ after the iteration of the proposed method run 281 times. From Figure 6, the Kriging predicted performance function $\widehat{g}(\mathbf{x})$ is almost consistent with $g(\mathbf{x})$ in the main domain, and most of the sample points' signs are right (Figure 7).

In order to demonstrate the efficiency of HPF, the active reliability method is tested with the different learning functions (such as EFF, ERF, U, and HPF). To avoid the effect of other random factors, EFF, ERF, U, and HPF are performed on the same Monte Carlo candidate points and initial DOE. Figure 8 shows the iterative graphs of $\widehat{p}_{\mathrm{f},\widehat{g}}/\widehat{p}_{\mathrm{f},g}$ corresponding to n_{call} by the different point-selected learning functions. By comparison, the convergence speed of HPF is faster than that of other learning functions, and HPF requires the least number of calls to the real performance function than other point-selected learning functions at the same precision level.

To demonstrate the influences of the different stopping criteria on the reliability results, $\min_{\mathbf{x}\in\mathbf{S}}(U(\mathbf{x})) \ge 2$, $P(C) \ge 0.99$ and the improved criterion equation (20) ($P_{\mathrm{threshold}} = 0.998$) are, respectively, applied in the active learning reliability methods. The results of different methods are listed in Table 1, where $\widehat{p}_{\mathrm{f}}$ is the estimated failure probability; δ is the coefficient of variation for the estimated failure probability; ε is the relative percentage error in comparison with the reference failure probability $\widehat{p}_{\mathrm{f},g}$ and it can be calculated by $\varepsilon = |\widehat{p}_{\mathrm{f}} - \widehat{p}_{\mathrm{f},g}|/\widehat{p}_{\mathrm{f},g}$; and n_{call} is the number of calls to the real performance function.

It can be seen from Table 1 that the failure probabilities obtained by three iteration termination criteria are all quite accurate. The result of the global stopping criterion $P(C) \ge$

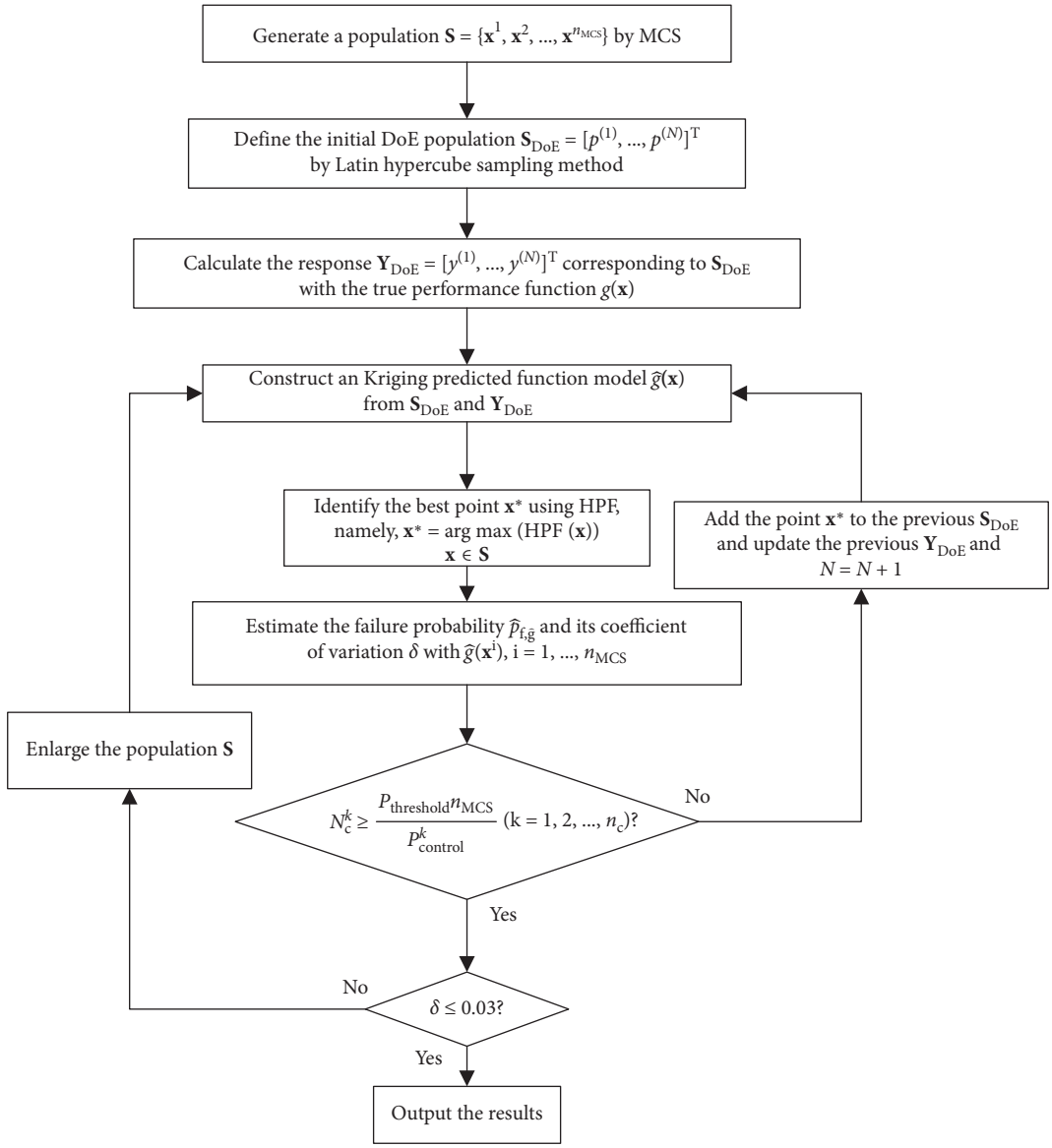

Figure 4: Procedure of the proposed reliability method.

0.99 is the most accurate one, and its relative error is almost 0. This is because $P(C) \geq 0.99$ is the most strict one. However, the improved stopping criterion requires the least number of calls to the real performance function among three criteria, whose relative errors are all less than 0.0028 ($\varepsilon \leq 0.00028$). Therefore, the improved stopping condition could get a relatively accurate result faster than others.

4.2. Case 2 (Multidimensional Performance Function). The second example is a multidimensional performance function, which is a classic illustration in [13, 25]. The explicit expression of the performance function is given as

$$g(c_1, c_1, m, r, t_1, F)_1 = 3r - \left|\frac{2F_1}{m\omega_0^2}\sin\left(\frac{\omega_0^2 t_1}{2}\right)\right|, \quad (23)$$

where $\omega_0 = \sqrt{c_1 + c_2/m}$. The means and standard deviations of the six random variables are listed in Table 2.

In order to demonstrate the efficiency of HPF, the active reliability method is tested with the different learning functions (such as EFF, ERF, U, and HPF). EFF, ERF, U, and HPF are performed on the same Monte Carlo candidate points and initial DOE. Figure 9 shows the iterative graphs of $\widehat{p}_{f,\widehat{g}}/\widehat{p}_{f,g}$ corresponding to n_{call} by the different point-selected learning functions. By comparison, the convergence speed of HPF is faster than that of other learning functions, and HPF requires the least number of calls to the real performance function than other point-selected learning functions at the same precision level.

To demonstrate the influences of the different stopping criteria on the reliability results, $\min_{\mathbf{x}\in\mathbf{S}}(U(\mathbf{x})) \geq 2$, $P(C) \geq 0.99$ and the improved criterion equation (20) ($P_{threshold} = 0.998$) are, respectively, applied in active learning reliability methods. The results of different methods are listed in Table 3, where $\widehat{p}_f$ is the estimated

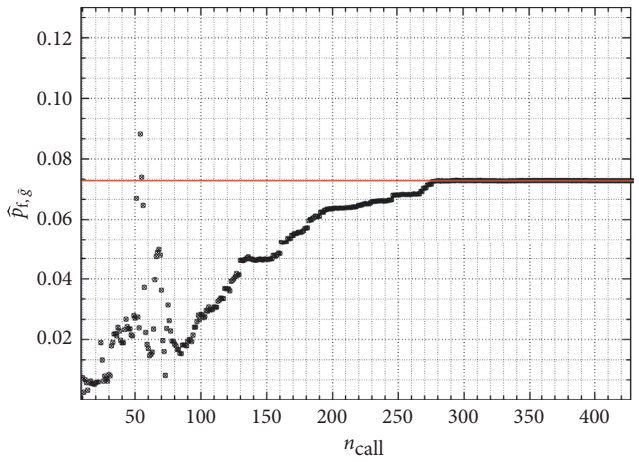

Figure 5: Graph of the failure probability.

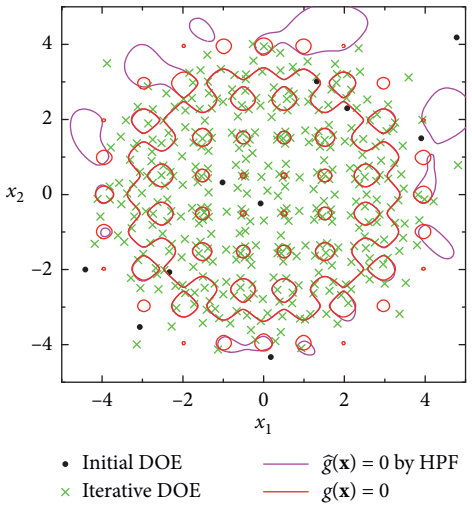

Figure 6: Predicted performance function and DOE points.

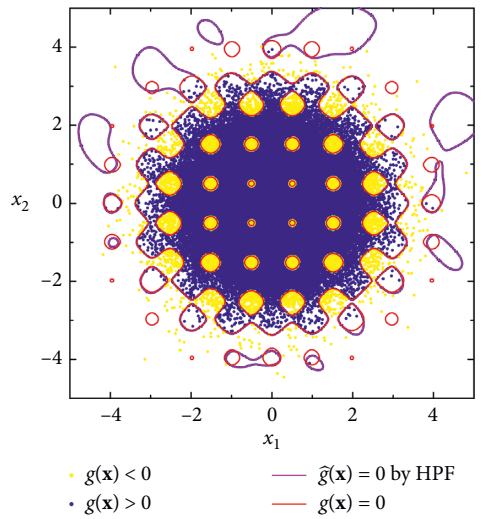

Figure 7: The sample points by MCS.

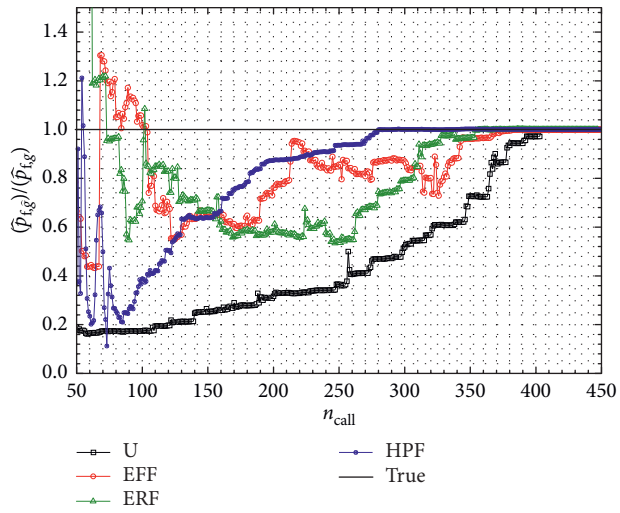

Figure 8: Iterative graphs of the $\widehat{p}_f$ with different point-selected learning functions.

failure probability; δ is the coefficient of variation for the estimated failure probability; ε is the relative percentage error in comparison with the reference failure probability $\widehat{p}_{f,g}$ and it can be calculated by $\varepsilon = |p_f - \widehat{p}_{f,g}|/\widehat{p}_{f,g}$; and n_{call} is the number of calls to the real performance function.

It can be seen from Table 3 that the failure probabilities obtained by three iteration termination criteria are all quite accurate. The result of the global stopping criterion $P(C) \geq 0.99$ is the most accurate one, and its relative error is almost 0. This is because $P(C) \geq 0.99$ is the most strict one. However, the improved stopping criterion requires the least number of calls to the real performance function among three criteria, whose relative errors are all less than 0.00104 ($\varepsilon \leq 0.00104$). Therefore, the improved stopping condition could get a relatively accurate result faster than others.

5. Application of Mechanical Reliability Analysis

Gear is one of the most important parts of the mechanical equipment. When the gears are engaged, the dynamic transmission error of the gear pair will be generated due to the random errors (such as manufacturing error and assembly error). Too large dynamic transmission error will cause the mechanical system to produce strong impact, vibration, and noise [26], so it is regarded as a failure mode of the gear transmission. In this section, the nonlinear vibration system (Figure 10) of a spur gear pair is set as the object of this study, and the proposed reliability method is applied to the reliability analysis of the gear vibration.

Table 1: Comparison of the $\widehat{p}_f$ values with different methods.

Reliability method					
Learning function	Stopping criterion	n_{call}	$\widehat{p}_f\,(10^{-2})$	δ	ε
	MCS	1×10^5	7.279	0.01128	—
HPF	$\min_{x\in S}(U(x))\geq 2$	418	7.279	0.01129	0.00000
	$P(C)\geq 0.99$	438	7.279	0.01129	0.00000
	Improved criterion	380	7.283	0.01128	0.00055
EFF	$\min_{x\in S}(U(\mathbf{x}))\geq 2$	447	7.278	0.01129	0.00014
	$P(C)\geq 0.99$	457	7.279	0.01129	0.00000
	Improved criterion	430	7.277	0.01129	0.00028
ERF	$\min_{x\in S}(U(\mathbf{x}))\geq 2$	431	7.279	0.01129	0.00000
	$P(C)\geq 0.99$	439	7.279	0.01129	0.00000
	Improved criterion	418	7.280	0.01129	0.00014
U	$\min_{x\in S}(U(\mathbf{x}))\geq 2$	433	7.279	0.01129	0.00000
	$P(C)\geq 0.99$	438	7.279	0.01129	0.00000
	Improved criterion	400	7.279	0.01129	0.00000

Table 2: Mean and standard deviation of all random variables.

Variable	Distribution type	Mean	Standard deviation
M	GAUSS	1	0.05
c_1	GAUSS	1	0.1
c_2	GAUSS	0.1	0.01
R	GAUSS	0.5	0.05
F_1	GAUSS	1	0.2
t_1	GAUSS	1	0.2

5.1. Response of the Gear. The differential equation of the gear vibration system is expressed as (the detailed procedure of derivation is seen in [27])

$$\begin{bmatrix}1&0&0\\0&1&0\\-1&1&1\end{bmatrix}\begin{Bmatrix}\dfrac{d^2y_p}{dt^2}\\[2ex]\dfrac{d^2y_g}{dt^2}\\[2ex]\dfrac{d^2y}{dt^2}\end{Bmatrix}+2\begin{bmatrix}\xi_p&0&\xi_{mp}\\0&\xi_g&-\xi_{mg}\\0&0&\xi_m\end{bmatrix}\begin{Bmatrix}\dfrac{dy_p}{dt}\\[2ex]\dfrac{dy_g}{dt}\\[2ex]\dfrac{dy}{dt}\end{Bmatrix}+\begin{bmatrix}k_{11}&0&k_{13}\\0&k_{22}&-k_{23}\\0&0&k_{33}\end{bmatrix}\begin{Bmatrix}f_p(y_p)\\f_g(y_g)\\f_m(y)\end{Bmatrix}=\begin{Bmatrix}0\\0\\F-\dfrac{d^2e}{dt^2}\end{Bmatrix},\tag{24}$$

where the parameters of equation (24) are expressed as follows: $y(t)=\overline{y}(\overline{t})/b$, $y_p(t)=\overline{y}_p(\overline{t})/b$, $y_g(t)=\overline{y}_g(\overline{t})/b$, $\xi_m=c_m/2m_e\omega_n$, $\xi_p=c_p/2m_p\omega_n$, $\xi_g=c_g/2m_g\omega_n$, $\xi_{mp}=c_m/2m_p\omega_n$, $\xi_{mg}=c_m/2m_g\omega_n$, $c_m=2\xi_m m_e\omega_n$, $e(t)=\overline{e}(\overline{t})/b$, $k_{11}=k_p/m_p\omega_n^2$, $k_{13}=k_m(\overline{t})/m_p\omega_n^2$, $k_{22}=k_g/m_g\omega_n^2$, $k_{23}=k_m(\overline{t})/m_g\omega_n^2$, $k_{33}=k_m(\overline{t})/m_e\omega_n^2$, and $F=\overline{F}/bm_e\omega_n^2$, where m_p and m_g are the masses of the gear and pinion, respectively, and m_e is the equivalent mass of the gear pair; k_p, k_g, and k_m are the stiffnesses corresponding to m_p, m_g, and m_e; $\overline{F}$ is the gear meshing force; $t=\overline{t}\omega_n$ is dimensionless time, in which t is the time; and $\omega_n=\sqrt{k_0/m_e}$ is the inherent frequency, where k_0 is the average value of the time-varying meshing stiffness between the gear and pinion. The static transmission error $e(t)$ is converted to a sine function with the Fourier series as $e(t)=\overline{e}(\overline{t})/b=\overline{e}_0/b+\overline{e}_r/b\sin(\omega_m t+\varphi)$. In the same way, $k_{13}(t)$, $k_{23}(t)$, and $k_{33}(t)$ is, respectively, expressed as $k_{13}(t)=k_m(\overline{t})/m_p\omega_n^2=m_e k_m(\overline{t})/m_p k_0=m_e/m_p+m_e/m_p\,\varepsilon\sin(\omega_m t+\varphi_k)$, $k_{23}(t)=k_m(\overline{t})/m_g\omega_n^2=m_e k_m(\overline{t})/m_g k_0=m_e/m_g+m_e/m_g\varepsilon\sin(\omega_m t+\varphi_k)$, $k_{33}(t)=k_m(\overline{t})/m_e\omega_n^2=k_m(\overline{t})/k_0=1+\varepsilon\sin(\omega_m t+\varphi_k)$.

The fourth-order Runge–Kutta numerical integration method edited by Matlab sofware is used to solve the vibration differential equation, and then the response of gear pair is obtained. It is noted that the process of computing the equation (24) is time-consuming and it requires about 7.260 seconds to calculate the implicit performance function.

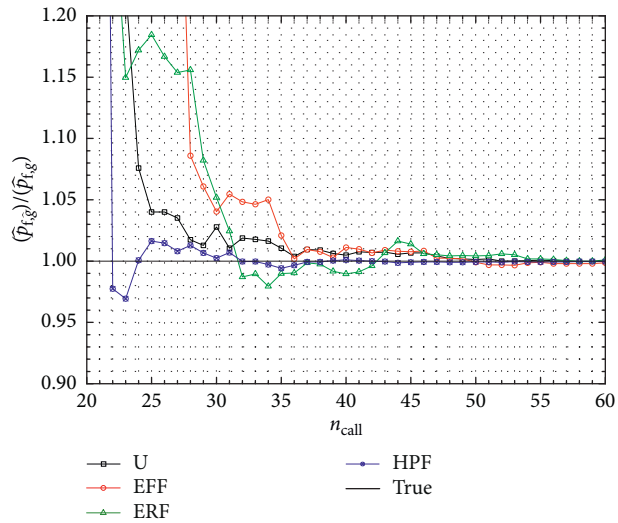

Figure 9: Iterative graphs of the $\widehat{p}_f$ with different point-selected learning functions.

Table 3: Comparison of the $\widehat{p}_f$ with different methods.

Reliability method		n_{call}	$\widehat{p}_f\,(10^{-2})$	δ	ε
Learning function	Stopping criterion				
	MCS	1×10^5	2.873	0.01839	—
	$\min_{\mathbf{x}\in\mathbf{S}}(U(\mathbf{x}))\geq 2$	58	2.872	0.01839	0.00035
HPF	$P(C)\geq 0.99$	65	2.873	0.01839	0.00000
	Improved criterion	36	2874	0.01838	0.00035
	$\min_{\mathbf{x}\in\mathbf{S}}(U(\mathbf{x}))\geq 2$	64	2.870	0.01840	0.00104
EFF	$P(C)\geq 0.99$	73	2.873	0.01839	0.00000
	Improved criterion	42	2.892	0.01832	0.00661
	$\min_{\mathbf{x}\in\mathbf{S}}(U(\mathbf{x}))\geq 2$	61	2.871	0.01839	0.00070
ERF	$P(C)\geq 0.99$	69	2.873	0.01839	0.00000
	Improved criterion	41	2.847	0.01847	0.00905
	$\min_{\mathbf{x}\in\mathbf{S}}(U(\mathbf{x}))\geq 2$	68	2.873	0.01839	0.00000
U	$P(C)\geq 0.99$	68	2.873	0.01839	0.00000
	Improved criterion	40	2.873	0.01839	0.00000

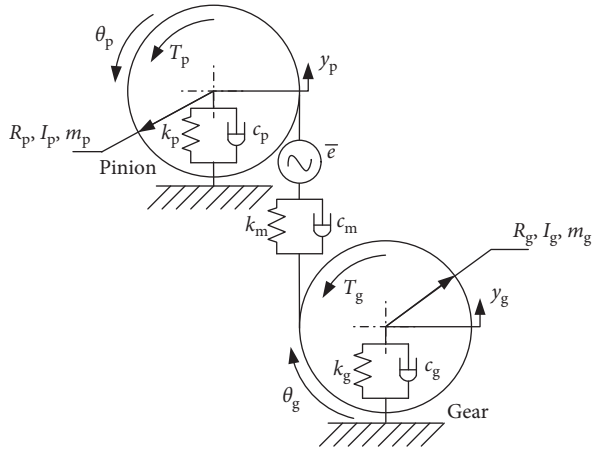

Figure 10: Nonlinear vibration system of a spur gear pair.

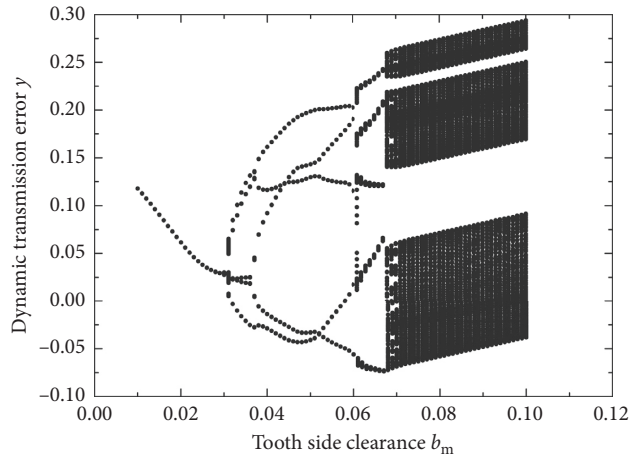

Figure 11: Bifurcation diagram.

Table 4: Mean and standard deviation of all variables.

Variable	Distribution type	Mean	Standard deviation
ε	Gauss	0.2	0.02
ξ_m	Gauss	0.1	0.02
b_m	Gauss	0.07	0.01
ω_m	Gauss	0.3	0.05

Furthermore, the response of this gear system is highly nonlinear.

5.2. Limit State Function of Gear Vibration. The meshing stiffness ε, meshing damping ξ_m, tooth side clearance b_m, and rotational speed ω_m of the gear vibration system are considered as random factors. According to [26], ε, ξ_m, b_m, and ω_m obey the Gauss distribution, and the means and standard deviations of all random variables are listed in Table 4.

If the fluctuation of the dynamic transmission error $y(t)$ exceeds the threshold value, the gear vibration system is in the failure state. Based on this failure mode, the performance function of the gear vibration system is expressed as

$$g(\mathrm{x}) = |y| - \Delta y, \tag{25}$$

where Δy is the fluctuation value of the dynamic transmission error, i.e., $\Delta y = y_{max} - y_{min}$, in which y_{max} and y_{min}, respectively, represent the maximum and minimum values of the dynamic transmission error during the engagement of the gear pair, namely, $y_{max} = \max\{y(t)\}$ and $y_{min} = \min\{y(t)\}$ and $|y|$ is the threshold value, which is selected as 0.055 mm in this paper. When $|y| > \Delta y$, $g(\mathbf{x}) > 0$, so the gear is in the safe state. When $|y| \leq \Delta y$, $g(\mathbf{x}) \leq 0$, and then the gear is in the failure state.

It is known from Section 5.1 that $y(t)$ is an implicit response and needs to be obtained by solving equation (25) with the fourth-order Runge–Kutta numerical integration method, so the performance function $g(\mathbf{x})$ is also an implicit response as well, and each calculation of the gear performance function requires about 7.260 seconds (i3 cpu). Furthermore, the response of the gear performance function is highly nonlinear. For example, Figure 10 is the bifurcation

Table 5: Comparison of different methods.

Method	n_{call}	$\widehat{p}_{\text{f}}$	ε	CPU time
MCS	1×10^5	1.406×10^{-2} ($\delta=0.0264$)	—	7.264×10^5 s
FORM [1]	45	4.339×10^{-4} ($\beta=3.33$)	0.9693	4.731×10^2 s
RSM + MCS [5]	500	1.650×10^{-3}	0.8832	4.150×10^3 s
HPF+$\min_{\mathbf{x}\in\mathbf{S}}(U(\mathbf{x}))\geq2$	303	1.404×10^{-2}	0.0014	2.412×10^3 s
HPF+$P(C)\geq0.99$	416	1.407×10^{-2}	0.0007	3.455×10^3 s
HPF + improved condition (the proposed method)	240	1.409×10^{-2}	0.0060	1.827×10^3 s

diagram of the gear vibration system's response corresponding to the tooth side clearance b_{m}. It is shown from Figure 11 that as the tooth side clearance b_{m} increases; firstly, the system's motion changes from single period ($b_{\text{m}}\in[0.01, 0.032]$) to five times period ($b_{\text{m}}\in[0.32, 0.061]$), and then it becomes the quasiperiodic motion ($b_{\text{m}}\in[0.061, 0.068]$); finally, it is to be the chaotic motion state. Namely, the motion behavior of this gear system is highly nonlinear. And, the performance function response of the gear vibration is very sensitive to the slight changes of the system's parameters.

Therefore, this is the type problem of mechanical reliability analysis which is time-consuming and nonlinear. Traditional mechanical reliability methods (such as MCS, FORM, and RSM) will become nonapplied because of the problems of large computation and low precision.

5.3. Results and Discussion. To validate the efficiency and correctness of the proposed method, the gear vibration reliability analysis is also performed by the traditional mechanical reliability methods (such as crude MCS, FORM [1], and RSM + MCS [5]) and the active learning reliability methods (such as HPF + $\min_{\mathbf{x}\in\mathbf{S}}(U(\mathbf{x}))\geq2$, HPF + $P(C)\geq0.99$, and HPF + improved condition ($P_{\text{threshold}}=0.99$)), where the result of the crude MCS is regarded as the true one; FORM is the first order second-moment reliability method; RSM + MCS means that the polynomial response surface based on Latin DOE is established, and then the constructed response surface is used to calculate the failure probability using MCS.

Table 5 shows the results of different methods. It can be found from Table 5 that FORM, RSM + MCS, HPF + $\min_{\mathbf{x}\in\mathbf{S}}(U(\mathbf{x}))\geq2$, HPF + $P(C)\geq0.99$, and HPF + improved condition cost the cuputime about 473.1 s, 4150 s, 2412 s, 3455 s, and 1827 s, respectively. The computational efficiency of FORM, RSM + MCS, and the active learning reliability methods (HPF + $\min_{\mathbf{x}\in\mathbf{S}}(U(\mathbf{x}))\geq2$, HPF + $P(C)\geq0.99$, and HPF + improved condition) can be acceptable in the engineering. But the results of RSM + MCS and FORM are totally different from those of the crude MCS, and their relative errors are 0.9693 and 0.8831, respectively, due to the highly nonlinear performance function. Table 5 also shows that the results of the active learning reliability methods are all consistent with that of crude MCS, and the number of calls to the real performance function require 303(15 + 288), 416(15 + 401), and 240(15 + 225), respectively. And, they cost only 2412 s, 3455 s, and 1827 s cuputime. In comparison with 7.264×10^5 s of the crude MCS, the proposed active learning reliability method can improve the efficiency and accuracy dramatically. Comparing with the two stopping criteria $\min_{\mathbf{x}\in\mathbf{S}}(U(\mathbf{x}))\geq2$ and $P(C)\geq0.99$, the improved stopping criterion requires the least number of calls to the real performance function among three criteria, and its accuracy is enough in the engineering ($\varepsilon=0.0060$). The improved stopping condition could get a relatively accurate result faster than others. And, it is more suitable for reliability analysis with a time-consuming performance function.

6. Conclusions

The aim of this study is to solve the problem of large computation and low precision for the mechanical reliability analysis which is time-consuming and nonlinear response. A Kriging-based active learning reliability method is presented in this paper. The efficiency of the Kriging-based active learning reliability method mainly depends on the proposed hybrid point-selected learning function (HPF) which is inspired by EFF, ERF, and U. The analytic expression of HPF is deduced by averaging the hybrid indicator throughout the real space. The uncertainty of HPF could measure the features like the sampling density, the probability to be wrongly predicted, and the local and global uncertainty close to the limit state. The new point-selected criterion can help select the next point effectively, and only a small number of true function evaluations are required to build an accurate Kriging performance function. The efficiency and correctness of HPF are validated by two explicit examples. Finally, the proposed method is applied to reliability analysis of the gear vibration (involving time-consuming and highly nonlinear response). By comparing with traditional mechanical reliability methods, the results show that the proposed method can solve the problems of large computation and low precision.

For many engineering problems, the response of the system is often calculated by the numerical method (time-consuming) and its behavior is usually highly nonlinear. The proposed active reliability method is independent of the gear reliability analysis and treats the system response as a black box. Thus, the proposed method can be also used to solve other engineering problems to perform reliability analysis.

Appendix

Derivation Process of Equation (16)

When $\widehat{g}(\mathbf{x}) \geq 0$, $E[\mathrm{RF}(g(\mathbf{x})) \cdot \mathrm{EF}(g(\mathbf{x}))]$ can be expressed analytically as

$$
\begin{aligned}
E[\mathrm{RF}(g(\mathbf{x})) \cdot \mathrm{EF}(g(\mathbf{x}))] &= \int_{-\varepsilon}^{0} [-(g(\mathbf{x}))][\varepsilon + (g(\mathbf{x}))] \frac{1}{s(\mathbf{x})} \varphi \\
&\quad \cdot \left(\frac{(g(\mathbf{x})) - (\widehat{g}(\mathbf{x}))}{s(\mathbf{x})} \right) d[g(\mathbf{x})] \\
&= -\int_{-\varepsilon}^{0} [\widehat{g}(\mathbf{x}) + s(\mathbf{x})Z][\varepsilon + \widehat{g}(\mathbf{x}) \\
&\quad + s(\mathbf{x})Z] \varphi(\mathbf{x}) d(\mathbf{x}), \\
Z &= \frac{g(\mathbf{x}) - \widehat{g}(\mathbf{x})}{s(\mathbf{x})} \\
&= -\int_{-\varepsilon}^{0} \{\widehat{g}(\mathbf{x})[\varepsilon + \widehat{g}(\mathbf{x})] + [s(\mathbf{x})[\varepsilon + \widehat{g}(\mathbf{x})] \\
&\quad + \widehat{g}(\mathbf{x}) s(\mathbf{x})] Z + s^2(\mathbf{x}) Z^2 \} \varphi(Z) d(Z) \\
&= -\int_{-\varepsilon - \widehat{g}(\mathbf{x})/s(\mathbf{x})}^{-\widehat{g}(\mathbf{x})/s(\mathbf{x})} \varphi(Z) d(Z) + [s(\mathbf{x}) \\
&\quad \cdot [\varepsilon + \widehat{g}(\mathbf{x})] + \widehat{g}(\mathbf{x}) s(\mathbf{x})] \\
&\quad \cdot \int_{-\varepsilon - \widehat{g}(\mathbf{x})/s(\mathbf{x})}^{-\widehat{g}(\mathbf{x})/s(\mathbf{x})} Z \varphi(Z) d(Z) + s^2(\mathbf{x}) \\
&\quad \cdot \int_{-\varepsilon - \widehat{g}(\mathbf{x})/s(\mathbf{x})}^{-\widehat{g}(\mathbf{x})/s(\mathbf{x})} Z^2 \varphi(Z) d(Z) \\
&= -\widehat{g}(\mathbf{x})[\varepsilon + \widehat{g}(\mathbf{x})] \Phi(Z) \Big|_{-\varepsilon - \widehat{g}(\mathbf{x})/s(\mathbf{x})}^{-\widehat{g}(\mathbf{x})/s(\mathbf{x})} \\
&\quad - [s(\mathbf{x})[\varepsilon + \widehat{g}(\mathbf{x})] + \widehat{g}(\mathbf{x}) s(\mathbf{x})] \\
&\quad \cdot \Phi(Z) \Big|_{-\varepsilon - \widehat{g}(\mathbf{x})/s(\mathbf{x})}^{-\widehat{g}(\mathbf{x})/s(\mathbf{x})} - s^2(\mathbf{x}) Z \varphi(Z) \\
&\quad \cdot \Big|_{-\varepsilon - \widehat{g}(\mathbf{x})/s(\mathbf{x})}^{-\widehat{g}(\mathbf{x})/s(\mathbf{x})} \\
&= -\left\{ \left[\widehat{g}(\mathbf{x})(-\varepsilon - \widehat{g}(\mathbf{x})) - s^2(\mathbf{x}) \right] \right. \\
&\quad \cdot \left[\Phi\left(\frac{-\varepsilon - \widehat{g}(\mathbf{x})}{s(\mathbf{x})} \right) - \Phi\left(\frac{-\widehat{g}(\mathbf{x})}{s(\mathbf{x})} \right) \right] \\
&\quad + \widehat{g}(\mathbf{x}) s(\mathbf{x}) \varphi\left(\frac{-\varepsilon - \widehat{g}(\mathbf{x})}{s(\mathbf{x})} \right) \\
&\quad \left. + s(\mathbf{x})(-\varepsilon - \widehat{g}(\mathbf{x})) \varphi\left(\frac{-\widehat{g}(\mathbf{x})}{s(\mathbf{x})} \right) \right\},
\end{aligned}
\tag{A.1}
$$

where $\varphi(\cdot)$ is the probability density function of the standard normal distribution.

In the same way, when $\widehat{g}(\mathbf{x}) < 0$, the expectation of $\mathrm{RF}(g(\mathbf{x})) \cdot \mathrm{EF}(g(\mathbf{x}))$ can be expressed analytically as

$$
\begin{aligned}
&E[\mathrm{RF}(g(\mathbf{x})) \cdot \mathrm{EF}(g(\mathbf{x}))] \\
&\quad = \int_{0}^{\varepsilon} [(g(\mathbf{x}))][\varepsilon - (g(\mathbf{x}))] \frac{1}{s(\mathbf{x})} \varphi \\
&\qquad \cdot \left(\frac{g(\mathbf{x}) - \widehat{g}(\mathbf{x})}{s(\mathbf{x})} \right) d[g(\mathbf{x})] \\
&\quad = \int_{0}^{\varepsilon} [\widehat{g}(\mathbf{x}) + s(\mathbf{x})Z][\varepsilon - \widehat{g}(\mathbf{x}) \\
&\qquad - s(\mathbf{x})Z] \varphi(Z) d(Z), \\
&\quad Z = \frac{g(\mathbf{x}) - \widehat{g}(\mathbf{x})}{s(\mathbf{x})} \\
&\quad = \int_{0}^{\varepsilon} \{\widehat{g}(\mathbf{x})[\varepsilon - \widehat{g}(\mathbf{x})] + [s(\mathbf{x}) \\
&\qquad \cdot [\varepsilon - \widehat{g}(\mathbf{x})] - \widehat{g}(\mathbf{x}) s(\mathbf{x})] Z \\
&\qquad - s^2(\mathbf{x}) Z^2 \} \varphi(Z) d(Z) \\
&\quad = \int_{-\widehat{g}(\mathbf{x})/s(\mathbf{x})}^{\varepsilon - \widehat{g}(\mathbf{x})/s(\mathbf{x})} \varphi(Z) d(Z) + [s(\mathbf{x}) \\
&\qquad \cdot [\varepsilon - \widehat{g}(\mathbf{x})] - \widehat{g}(\mathbf{x}) s(\mathbf{x})] \\
&\qquad \cdot \int_{-\widehat{g}(\mathbf{x})/s(\mathbf{x})}^{\varepsilon - \widehat{g}(\mathbf{x})/s(\mathbf{x})} Z \varphi(Z) d(Z) - s^2(\mathbf{x}) \\
&\qquad \cdot \int_{-\widehat{g}(\mathbf{x})/s(\mathbf{x})}^{\varepsilon - \widehat{g}(\mathbf{x})/s(\mathbf{x})} Z^2 \varphi(Z) d(Z) \\
&\quad = \widehat{g}(\mathbf{x})[\varepsilon - \widehat{g}(\mathbf{x})] \Phi(Z) \Big|_{-\widehat{g}(\mathbf{x})/s(\mathbf{x})}^{\varepsilon - \widehat{g}(\mathbf{x})/s(\mathbf{x})} \\
&\qquad - [s(\mathbf{x})[\varepsilon - \widehat{g}(\mathbf{x})] - \widehat{g}(\mathbf{x}) s(\mathbf{x})] \\
&\qquad \cdot \Phi(Z) \Big|_{-\widehat{g}(\mathbf{x})/s(\mathbf{x})}^{\varepsilon - \widehat{g}(\mathbf{x})/s(\mathbf{x})} + s^2(\mathbf{x}) Z \varphi(Z) \Big|_{-\widehat{g}(\mathbf{x})/s(\mathbf{x})}^{\varepsilon - \widehat{g}(\mathbf{x})/s(\mathbf{x})} \\
&\quad = \left[\widehat{g}(\mathbf{x})(\varepsilon - \widehat{g}(\mathbf{x})) - s^2(\mathbf{x}) \right] \\
&\qquad \left[\Phi\left(\frac{\varepsilon - \widehat{g}(\mathbf{x})}{s(\mathbf{x})} \right) - \Phi\left(\frac{-\widehat{g}(\mathbf{x})}{s(\mathbf{x})} \right) \right] \\
&\qquad + \widehat{g}(\mathbf{x}) s(\mathbf{x}) \varphi\left(\frac{\varepsilon - \widehat{g}(\mathbf{x})}{s(\mathbf{x})} \right) \\
&\qquad + s(\mathbf{x})(\varepsilon - \widehat{g}(\mathbf{x})) \varphi\left(\frac{-\widehat{g}(\mathbf{x})}{s(\mathbf{x})} \right).
\end{aligned}
\tag{A.2}
$$

Equations (A.1) and (A.2) can be written into a uniform expression as

$$E[\mathrm{RF}(g(\mathbf{x}))\cdot \mathrm{EF}(g(\mathbf{x}))] = -\mathrm{sign}(\widehat{g}(\mathbf{x}))\Bigg\{[\widehat{g}(\mathbf{x}) \cdot (-\varepsilon \mathrm{sign}(\widehat{g}(\mathbf{x})) - \widehat{g}(\mathbf{x}))s(\mathbf{x})] \cdot \left[\Phi\left(\frac{-\varepsilon \mathrm{sign}(\widehat{g}(\mathbf{x})) - \widehat{g}(\mathbf{x})}{s(\mathbf{x})}\right) - \Phi\left(\frac{-\widehat{g}(\mathbf{x})}{s(\mathbf{x})}\right)\right] + \widehat{g}(\mathbf{x})s(\mathbf{x})\varphi \cdot \left(\frac{-\varepsilon \mathrm{sign}(\widehat{g}(\mathbf{x})) - \widehat{g}(\mathbf{x})}{s(\mathbf{x})}\right) + s(\mathbf{x})[-\varepsilon \mathrm{sign}(\widehat{g}(\mathbf{x})) - \widehat{g}(\mathbf{x})]\varphi\left(\frac{-\widehat{g}(\mathbf{x})}{s(\mathbf{x})}\right)\Bigg\}, \tag{A.3}$$

where $\mathrm{sign}(\cdot)$ is the sign function and $\mathrm{sign}(\widehat{g}(\mathbf{x})) = \begin{cases} 1, & \widehat{g}(\mathbf{x}) \geq 0, \\ -1, & \widehat{g}(\mathbf{x}) < 0. \end{cases}$

Derivation completed.

Data Availability

The data of the active learning algorithm are available from the corresponding author upon request. However, the application data of this research cannot be valid because the application example in this paper is based on the background of the national aerospace field, which involves some confidential data.

Conflicts of Interest

The authors declare that they have no conflicts of interest.

Acknowledgments

This research was financially supported by the Young Doctor Scientific Research Foundation of College (Grant no. 19YB27), State Key Laboratory of Robotics (Grant no. 2017-Z18), and Liaoning Provincial Natural Science Foundation (Grant no. 2018010334-301). Their financial supports are gratefully acknowledged.

References

[1] M. D. McKay, R. J. Beckman, and W. J. Conover, "Comparison of three methods for selecting values of input variables in the analysis of output from a computer code," *Technometrics*, vol. 21, no. 2, pp. 239–245, 1979.

[2] R. E. Caflisch, "Monte Carlo and quasi-Monte Carlo methods," *Acta Numerica*, vol. 7, pp. 1–49, 1998.

[3] S. K. Au and J. L. Beck, "Important sampling in high dimensions," *Structural Safety*, vol. 25, no. 2, pp. 139–163, 2003.

[4] I. Kaymaz, "Application of Kriging method to structural reliability problems," *Structural Safety*, vol. 27, no. 2, pp. 133–151, 2005.

[5] V. J. Romero, L. P. Swiler, and A. A. Giunta, "Construction of response surfaces based on progressive-lattice-sampling experimental designs with application to uncertainty propagation," *Structural Safety*, vol. 26, no. 2, pp. 201–219, 2004.

[6] J. Cheng, "Hybrid genetic algorithms for structural reliability analysis," *Computers & Structures*, vol. 85, no. 19-20, pp. 1524–1533, 2007.

[7] T. H. Lee and J. J. Jung, "A sampling technique enhancing accuracy and efficiency of metamodel-based RBDO: constraint boundary sampling," *Computers & Structures*, vol. 86, no. 13-14, pp. 1463–1476, 2008.

[8] B. Gaspar, A. P. Teixeira, and C. G. Soares, "Assessment of the efficiency of Kriging surrogate models for structural reliability analysis," *Probabilistic Engineering Mechanics*, vol. 37, pp. 24–34, 2014.

[9] X. Shi, Â. Palos Teixeira, J. Zhang, and C. Guedes Soares, "Kriging response surface reliability analysis of a ship-stiffened plate with initial imperfections," *Structure and Infrastructure Engineering*, vol. 11, no. 11, pp. 1450–1465, 2015.

[10] D. R. Jones, M. Schonlau, and W. J. Welch, "Efficient global optimization of expensive black-box functions," *Journal of Global Optimization*, vol. 13, no. 4, pp. 455–492, 1998.

[11] B. J. Bichon, M. S. Eldred, L. P. Swiler, S. Mahadevan, and J. M. McFarland, "Efficient global reliability analysis for nonlinear implicit performance functions," *AIAA Journal*, vol. 46, no. 10, pp. 2459–2468, 2008.

[12] B. J. Bichon, J. M. McFarland, and S. Mahadevan, "Efficient surrogate models for reliability analysis of systems with multiple failure modes," *Reliability Engineering & System Safety*, vol. 96, no. 10, pp. 1386–1395, 2011.

[13] B. Echard, N. Gayton, and M. Lemaire, "AK-MCS: an active learning reliability method combining Kriging and Monte Carlo Simulation," *Structural Safety*, vol. 33, no. 2, pp. 145–154, 2011.

[14] B. Echard, N. Gayton, M. Lemaire, and N. Relun, "A combined importance sampling and Kriging reliability method for small failure probabilities with time-demanding numerical models," *Reliability Engineering & System Safety*, vol. 111, pp. 232–240, 2013.

[15] X. Yang, Y. Liu, Y. Gao, Y. Zhang, and Z. Gao, "An active learning Kriging model for hybrid reliability analysis with both random and interval variables," *Structural and Multidisciplinary Optimization*, vol. 51, no. 5, pp. 1003–1016, 2015.

[16] Z. Wen, H. Pei, H. Liu, and Z. Yue, "A Sequential Kriging reliability analysis method with characteristics of adaptive sampling regions and parallelizability," *Reliability Engineering & System Safety*, vol. 153, pp. 170–179, 2016.

[17] C. Tong, Z. Sun, Q. Zhao, Q. Wang, and S. Wang, "A hybrid algorithm for reliability analysis combining Kriging and subset simulation importance sampling," *Journal of Mechanical Science and Technology*, vol. 29, no. 8, pp. 3183–3193, 2015.

[18] F. Cadini, F. Santos, and E. Zio, "An improved adaptive Kriging-based importance technique for sampling multiple failure regions of low probability," *Reliability Engineering & System Safety*, vol. 131, pp. 109–117, 2014.

[19] W. Fauriat and N. Gayton, "AK-SYS: an adaptation of the AK-MCS method for system reliability," *Reliability Engineering & System Safety*, vol. 123, pp. 137–144, 2014.

[20] X. Yang, Y. Liu, Y. Zhang, and Z. Yue, "Probability and convex set hybrid reliability analysis based on active learning

Kriging model," *Applied Mathematical Modelling*, vol. 39, no. 14, pp. 3954–3971, 2015.

[21] Z. Lv, Z. Lu, and P. Wang, "A new learning function for Kriging and its applications to solve reliability problems in engineering," *Computers & Mathematics with Applications*, vol. 70, no. 5, pp. 1182–1197, 2015.

[22] Z. Sun, J. Wang, R. Li, and C. Tong, "LIF: a new Kriging based learning function and its application to structural reliability analysis," *Reliability Engineering & System Safety*, vol. 157, pp. 152–165, 2017.

[23] J. Wang and Z. Sun, "The stepwise accuracy-improvement strategy based on the Kriging model for structural reliability analysis," *Structural and Multidisciplinary Optimization*, vol. 58, no. 2, pp. 595–612, 2018.

[24] J. Wang, Z. Sun, Q. Yang, and R. Li, "Two accuracy measures of the Kriging model for structural reliability analysis," *Reliability Engineering & System Safety*, vol. 167, pp. 494–505, 2017.

[25] N. Lelièvre, P. Beaurepaire, C. Mattrand, and N. Gayton, "AK-MCSi: a Kriging-based method to deal with small failure probabilities and time-consuming models," *Structural Safety*, vol. 73, pp. 1–11, 2018.

[26] Z. L. Sun and L. Y. Chen, *Practical Mechanical Reliability Design Theory and Method*, Science Press, Shanghai, China, 2003.

[27] R. Li and J. Wang, *Dynamics of Gear System*, Science Press, Shanghai, China, 1997.